Responses to Reviewer #1

General Comments:
Zang & Willis present an instrument characterization study of a Vocus CIMS, switching between H3O+ and NH4+ reagent ions for the purpose of detecting and quantifying a large range of reactive organic carbon compounds with a single CIMS. They investigate and optimize their ion-molecule reactor conditions for each reagent, present methodologies for quantifying hysteresis timescales when switching reagents, and demonstrate their capabilities via ambient measurements of fresh and oxidized biogenic emissions. I believe this manuscript will serve as a solid foundation for new Vocus users who aim to use reagent switching. Many of my specific comments are meant to clarify details for such readers. I recommend this manuscript for publication following edits in response to the following comments.

Specific Comments:
Line 9 – Specify the integration time for the LODs (I believe 1 s?)
The reviewer is correct that these LODs are given at 1Hz. This information has been added.

Line 74 – The back reaction can also be important if the reaction is only slightly exothermic (e.g., HCHO in PTR).
We appreciate the importance of this detail. We revised this sentence accordingly: *"unless reaction timescales are long or the reaction is endothermic or only slightly exothermic."*

Line 110 – Specify the model of Vocus.
This information (Vocus-S) has been added.

Section 2.1 – Please include your fIMR and BSQ settings (amplitude and frequency) since they will also influence your sensitivities.
We now include this information along with a full list of instrument settings as Table S1 in the supplement. Additionally we have added the fIMR and BSQ settings in sections 2.3, 2.5, and 2.6 in the revised manuscript.

Line 127 – Rather than have the reader rely on the figures, list the full ranges of fIMR pressure and front voltage used in your experiments here as well. Also provide the corresponding, nominal E/N range.
We have added two sentences at the end of Sect. 2.2 that read: *"With NH_4^+, we characterized from 2.5 to 3.5 mbar and from 45 to 65 V cm-1 (60-120 Townsends (Td)). For H_3O^+, we characterized from 1.5 to 2.5 mbar and from 45 to 65 V cm-1 (80-200 Td)."*

Line 137 – Please provide the nominal E/N for each set of parameters.
This information has been added, see our response to the previous comment.

Section 2.3 – When calculating sensitivities, did you observe / account for interfering ions? For example, I find that the monoterpenes, including limonene, fragment to the C7H9+, toluene's quantitative ion.
Our calibration cylinders are composed to avoid interference from fragmentation as much as possible, though we did not make this clear in the original manuscript. To address this we have included a table in the supplement (Table S2) with information on the three different cylinders used in Section 2.3. We have also added the following sentence: *"The 23 analytes come from three separate multi-component cylinders where the composition was selected to avoid interferences from fragments (Table S2)."* Specifically, monoterpenes and toluene are not in the same cylinder, so we avoid monoterpene fragmentation to $C_7H_9^+$ during calibration.

Section 2.3 – A table in the SI with the observed fragments (and their abundances) would be useful for others attempting to characterize their own instrument.
We agree entirely that this information is important to include. Table S6 has been added with information on fragmentation patterns shown in Fig. 3. We have also added the following to the Fig. 3 caption: *"Data represented in this figure is shown in Table S6."*

Section 2.3 – Were any of the fragments you observed affected by the BSQ transmission attenuation? If so, did you correct for mass transmission when calculating fragmentation rates?
The smallest fragment we detect here is $C_5H_7^+$, which has an m/z of 67 and is above the BSQ mass filter range at 270V amplitude (Krechmer et al., 2018). For this reason we do not correct for mass transmission when calculating fragmentation rates.

Section 2.3 – In my experience, fragmentation seems to have a significant dependence on voltage gradients throughout the instrument (e.g., between the Vocus back voltage and the BSQ skimmer; or that same skimmer and the BSQ front voltage) in addition to the fIMR conditions. Have you investigated this dependence? If not, it may be prudent to note some of those gradients in your optimized setups for anyone attempting to recreate those conditions.
We agree entirely, and this information is now available in Table S1.

Section 2.3 – Was there a reason you settled on 60 °C (PTR is typically higher, 80-100 °C)? To promote NH4+ adducts? Higher temperatures are commonly used to limit adsorption, so would higher temperatures improve the hysteresis timescales?
Yes, we use 60 °C fIMR temperature to promote NH_4^+ adduct formation. We added a sentence acknowledging that this is different than traditional PTR conditions, and direct the reader to Section 3.1 where we discuss this choice in detail: *"Using a 60 °C reaction chamber with H_3O^+ is lower than commonly reported in the literature (∼80-100 °C) (e.g., Vermeuel et al., 2023; Coggon et al., 2024); this choice arises from fIMR temperature constraints for NH_4^+ (Xu et al., 2022) and is discussed in more detail in Sect. 3.1."*

Line 170 – Which ion optics do you change? I don't believe there is any discussion of changing e.g., BSQ or PB settings in Section 3.1 or the methods. From line 315 ("... changes in the BSQ mass range") it sounds like there was a change, unless I'm misunderstanding.
We change a number of ion optics upon a switch in reagent-ion including the BSQ and other downstream voltages. This information is now included in Table S1.

Section 3.3 – You note humidity independence based on your results. Broadly, I agree. However, I highly encourage addition discussion of the minor humidity dependence at the highest humidities as shown in Fig. 4 (NH4+ ∼5% higher at 50% RH, ∼10% higher at 70+% RH – except for alkenes). NH4+ appears to have a stronger dependence than H3O+? Can you comment on compound-related trends?
We appreciate this suggestion and have now added the following sentences discussing the mild humidity dependencies with both reagent ions: *"Varying sample humidity with constant analyte concentration demonstrates low humidity dependence with both NH_4^+ and H_3O^+ ionization across a range of reduced and oxygenated ROC (Fig. 4). We note an approximately 10 % increase in the NH_4^+ sensitivity to nitriles and oxygenates while alkene sensitivities remain unchanged up to 85 % RH. We also observe a slight (5-10%) increase in sensitivity with humidity for oxygenated species with H_3O^+, while alkene sensitivities are less affected. The low humidity dependence of the Vocus-CI-ToFMS has been demonstrated previously for H_3O^+ for a variety of analytes (Krechmer et al., 2018; Kilgour et al., 2022; Li et al., 2024) and for a select number of small oxygenates, alkenes, and acetonitrile with NH_4^+ (Khare et al., 2022; Xu et al., 2022). We demonstrate the low dependence of sensitivity on sample humidity with NH_4^+ ionization under different instrumental conditions and for a selection of analytes including oxygenated alkenes and siloxanes (Fig. 4)."*

Line 318 – The analyte ion was chosen due to persistence, but does it provide a representative hysteresis timescale for most/all analytes? Have you attempted to repeat this process with other analytes and do they yield similar results? Are there other considerations readers should be aware of when picking analytes/internal standards?
Our intention in the using C_3H_6O-ammonium analyte ion was to demonstrate that this method is feasible given a persistent ambient ion signal is available. However, we did not intend to suggest that other users should necessarily apply this specific product ion to diagnose hysteresis. While we alluded to the pitfalls of this approach in the original manuscript, and noted that more ideal tracer ions would involve the use of an internal standard (Preprint Line 321: *"Despite this, future iterations of this approach would benefit from applying our method on the signal from an internal standard infused into the sampling inlet."*), we agree

entirely that this aspect of our manuscript should be strengthened. To do this, we have added analysis of ambient switching data from another campaign, in which we infused a deuterated internal standard mixture directly into our inlet. This revision necessitated including an additional figure (Fig. 6 in the revised manuscript, here as Fig. AC1) and the addition of a new methods Section 2.6 including information about this deployment. We have revised Section 3.4 into two sections, which focus on diagnosing the timescales of reagent-ion hysteresis when only reagent ions and potentially persistent ambient ions are available, and when an internal standard is available. Notably, the deployment for which we used an internal standard occurred in a marine environment, and as a result the ambient C_3H_6O-ammonium analyte ion is not persistent enough to allow a direct comparison with our analysis from MEFO. The hysteresis timescales of 2-hexanone-d_4 and the C_3H_6O-ammonium adduct are comparable between the two campaigns. For NH_4^+ ionization, 2-hexanone-d_4 has a hysteresis time of 34 s during ARTofMELT, compared to the C_3H_6O-ammonium timescale of 75 s during MEFO. For H_3O^+ ionization, 2-hexanone-d_4 has a hysteresis time of 168 s during ARTofMELT, compared the the C_3H_6O-ammonium timescale of 185 s during MEFO. Overall, major considerations for selecting a ion to diagnose reagent-ion hysteresis are: m/z above the BSQ mass filter, persistence and stability. In the revised Section 3.4 we have highlighted this set of key considerations.

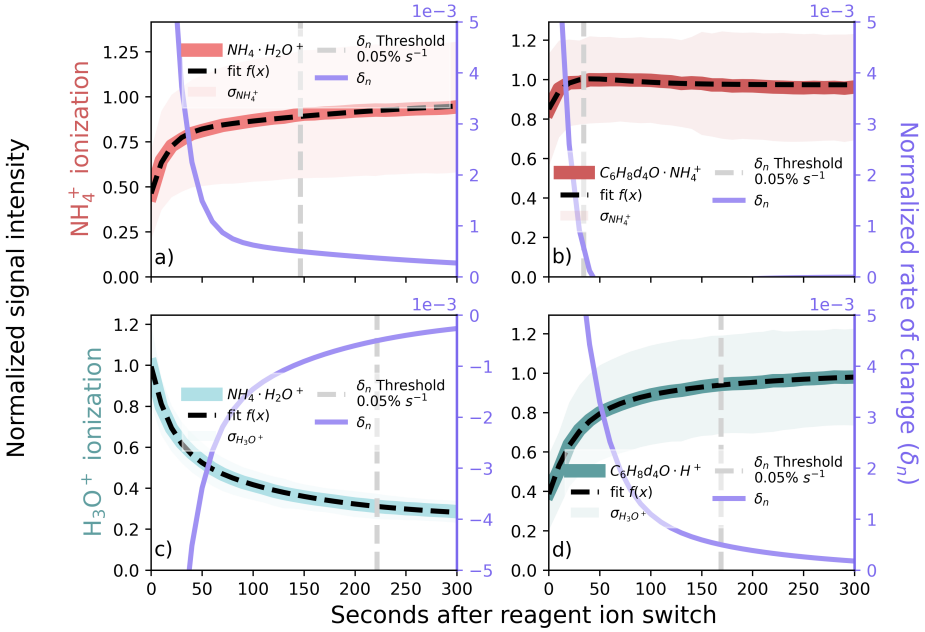

Figure AC1: Ion signal after a reagent-ion switch for NH_4^+ (a & b) and H_3O^+ (c & d) in the ARTofMELT data, showing $NH_4 \cdot H_2O^+$ ions (a & c), $C_6H_8d_4O \cdot NH_4^+$ (b) and $C_6H_8d_4O \cdot H^+$ (d) internal standard ions. We grouped ion signals by the time after a switch and normalized the mean of each group by the maximum, and normalized means were fit with a bi-exponential function. The derivative of the fit (δ_n) is displayed on the right axes (purple traces) and is used as a metric to filter reagent-ion hysteresis.

Line 319 – You mention that ambient variability may impact the derivation of hysteresis timescales. Have you performed the calculation in the absence of averaging (i.e., calculate the timescale for each reagent switch individually) to get a sense of the variability? If I were to apply the average hysteresis timescale to the whole campaign, is there a concern that some switches would have longer timescales that impact interpretability? We have incorporated an analysis of switch by switch variability in the supplement as Fig. S6 (Here as Fig. AC2). This analysis involved fitting traces after each switch with a bi-exponential fit and determining the time at which the derivative reached our 0.05 % s^{-1} threshold. The results demonstrate that the mean cutoff from the analysis in Sect. 3.4 (dashed lines with dark background in Fig. AC2) does not entirely capture the variability in hysteresis timescales for the majority of individual switches. We have added the following discussion to address this: *"A switch-by-switch analysis of hysteresis from MEFO (available as Fig. S6) shows that the 0.05 % s^{-1} δ_n cutoffs for $C_3H_6O{\cdot}NH_4^+$ calculated in Fig. 5b, d do not capture the majority of*

the switch-by-switch cutoffs (37 % for NH_4^+ and 39 % for H_3O^+). Therefore, if a persistent ambient ion is used to diagnose hysteresis timescales, this should be done on a switch-by-switch basis. This variability may be associated with ambient variations in the $C_3H_6O{\cdot}NH_4^+$ signal which can be avoided by applying our method described in Fig. 5 to a persistent and known signal from an internal standard (Sect. 3.4.2).” Results of the switch-by-switch analysis differ when we use the signal of an internal standard to monitor hysteresis during ARTofMELT (Fig. AC1), where the cutoffs calculated in Fig AC1 for 2-hexanone-d_4 capture 75 % of the switch-by-switch variability for NH_4^+ and 72 % for H_3O^+. (Fig. AC3)

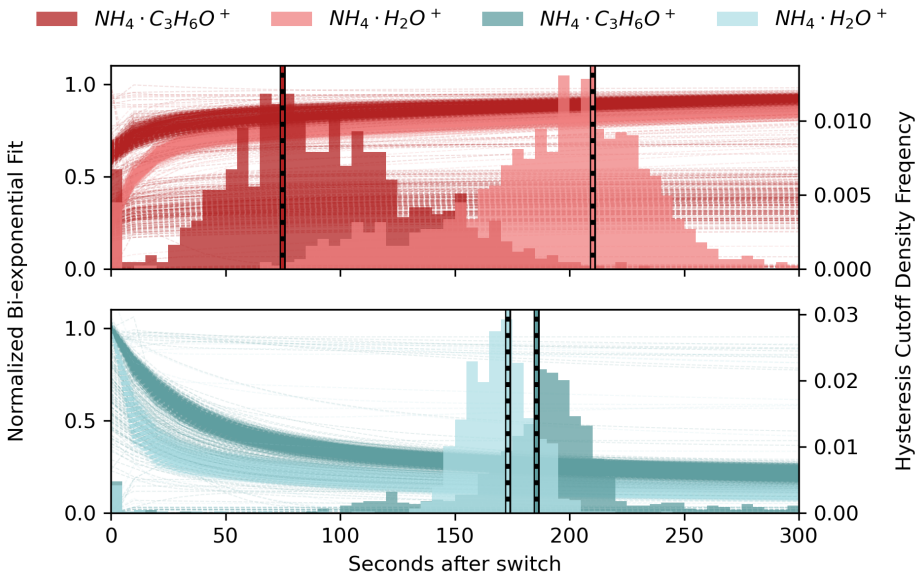

Figure AC2: Traces of bi-exponential fit for individual switches with NH_4^+ ionization (top) and H_3O^+ ionization (bottom) as well as a histogram of the time at which a 0.05 % s^{-1} change threshold is reached across individual switches. Dashed lines with black background show the cutoff from the average analysis used in Sect. 3.4. Data is from the MEFO.

Line 323 – Do you have recommendations for reagent switching timescales? Can you comment on striking a balance between rapid switching to monitor more ROC vs longer dwell times to minimize the data loss to hysteresis?
We have used 15 minute switching during multiple deployments with this method, and this has allowed for reasonable data coverage with both reagent ions. However, this could be adjusted depending on the timescales relevant to different sampling applications. For an example the ARTofMELT analysis with a deuterated internal standard resulted in 4% data loss for NH_4^+ and 19% data loss for H_3O^+ during 15 minute switching. Since the time of hysteresis would likely remain relatively constant, if a user were to decrease the switching timescale to 5 minutes this would yield 12% data loss with NH_4^+ and 57% data loss with H_3O^+. Depending on the application, this trade-off off data coverage and time resolution might be appropriate. Alternatively, with 30 minute switches these reagent-ion hysteresis timescales would result in 2% data loss with NH_4^+ and 10% data loss for H_3O^+. Selection of switching timescales, and balancing data coverage and time-resolution, should be optimized based on the experiment. Our aim here is to provide a quantitative method to diagnosing these timescale such that future users can make informed decisions for their application.

Lines 324-325 & Fig. 5e – Figure 5e took a while to understand. I kept trying to compare it to the purple traces in Fig. 5a-d. I think additional explanation in Section 3.4 on how to interpret Figure 5e would be beneficial for the reader.
Our goal with Fig. 5e was to provide information on the impact of adjusting the δ_n threshold above and below 0.05 % s−1. Your comparison to the purple traces in Fig. 5a-d is justified, as Figure 5e is essentially

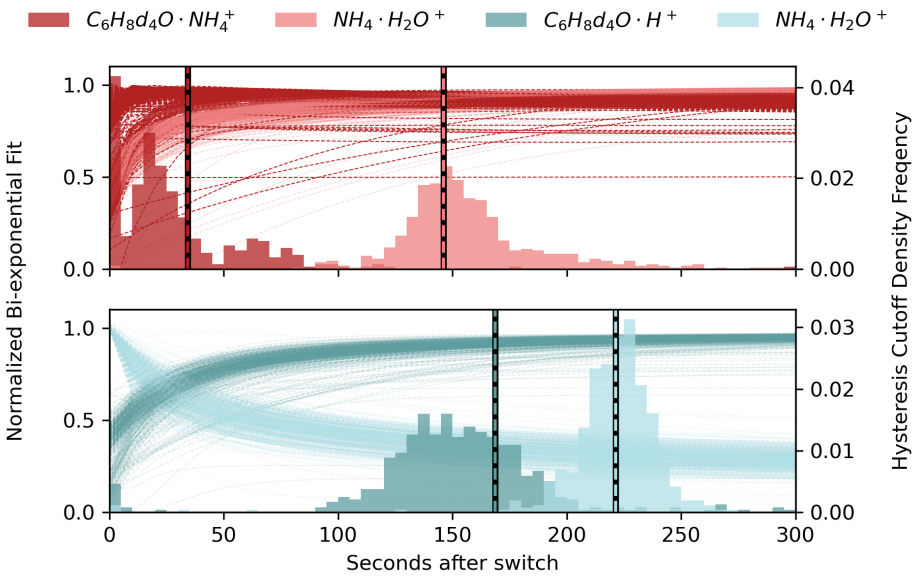

Figure AC3: Traces of bi-exponential fit for individual switches with NH_4^+ ionization (top) and H_3O^+ ionization (bottom) as well as a histogram of the time at which a 0.05 % s^{-1} change threshold is reached across individual switches. Dashed lines with black background show the cutoff from the average analysis used in Sect. 3.4. Data is from a 2-week period of the ARTofMELT expedition.

depicting the purple traces from Fig. 5a-d on a 900 s timescale. Based on the reviewer's comment, we found this panel to be somewhat redundant and likely confusing for the reader. We have chosen to move Figure 5e to the supplement, and refer to it when we discuss the sensitivity of data loss to the magnitude of the normalized rate-of-change threshold.

Line 326 – Also provide the % data lost for each reagent, since it is asymmetric.
This information has been added.

Line 404-405 – Reiterate the threshold you used here. Also note the data retention for each ion chemistry due to the different timescales.
We have moved this discussion into Sect. 3.4 in the revised manuscript with additional details on the reagent-ion dependent data retention. We've included the following text in the conclusions section reiterating the threshold we used and the data retention: *"To diagnose and quantify the timescales for reagent-ion switching hystersis we compare the use of three ion-types: NH_4^+ reagent ions; a persistent ambient NH_4^+-adduct ion; and NH_4^+-adduct or proton-transfer molecular ions from an internal standard infused in the sampling inlet. Reagent-ion signal variability at each switch is driven largely by changes in ion transmission so is less representative of ion chemistry, while monitoring a product ion is more directly related to ionization reactions taking place in the fIMR. An internal standard signal provides the ideal means to monitor reagent-ion hysteresis with a known and persistent product ion; however, persistent ambient ions and internal standard product ions can produce similar rates of data retention (~86-89 % data retention across a full 1800 s switching cycle with a 0.05 % s^{-1} rate-of-change threshold)."*

Figure 3 – The background shading is distracting. It took me a moment to realize they didn't represent data. I think the color coding of the standards' names is sufficient.
The background shading has now been removed from Fig. 3.

Figure 3 – I would typically associate "Molecular Ion Fraction" with A*H+ and A*NH4+ (i.e., inaccurate terminology for the fragments and clusters). Perhaps something closer to "Fractional Signal Contribution"?

We appreciate this suggestion and we have implemented the phrase "Fractional Signal Contribution" over Molecular ion fraction in the revised manuscript to be more general, as Figure 3 shows both molecular ions and fragment ions.

Figure 6 – How many ions are included in this plot?
There are a total of 725 ions in this figure. This information has been added to the figure legend of Fig. 7 in the revised manuscript.

Table S3 – Specify sensitivities are for NH4+.
The table caption now clarifies that these are sensitivities for NH_4^+.

Figure S4 – Expand the H3O+ panel y-axis so the dashed lines are more apparent.
The y-axis of this figure (which is Fig. S11 in the revised document manuscript) is now expanded.

Technical Comments:
Line 282 – Capitalize first word.
We have capitalized the first word to read "Reagent-ion".

References

M. M. Coggon, C. E. Stockwell, M. S. Claflin, E. Y. Pfannerstill, L. Xu, J. B. Gilman, J. Marcantonio, C. Cao, K. Bates, G. I. Gkatzelis, A. Lamplugh, E. F. Katz, C. Arata, E. C. Apel, R. S. Hornbrook, F. Piel, F. Majluf, D. R. Blake, A. Wisthaler, M. Canagaratna, B. M. Lerner, A. H. Goldstein, J. E. Mak, and C. Warneke. Identifying and correcting interferences to PTR-ToF-MS measurements of isoprene and other urban volatile organic compounds. *Atmospheric Measurement Techniques*, 17(2):801–825, Jan. 2024. ISSN 1867-8548. doi: 10.5194/amt-17-801-2024. URL `https://amt.copernicus.org/articles/17/801/2024/`.

P. Khare, J. E. Krechmer, J. E. Machesky, T. Hass-Mitchell, C. Cao, J. Wang, F. Majluf, F. Lopez-Hilfiker, S. Malek, W. Wang, K. Seltzer, H. O. T. Pye, R. Commane, B. C. McDonald, R. Toledo-Crow, J. E. Mak, and D. R. Gentner. Ammonium-adduct chemical ionization to investigate anthropogenic oxygenated gas-phase organic compounds in urban air. *Atmos Chem Phys*, 22(21):14377–14399, 2022. ISSN 1680-7316 (Print) 1680-7324 (Electronic) 1680-7316 (Linking). doi: 10.5194/acp-22-14377-2022. URL `https://www.ncbi.nlm.nih.gov/pubmed/36506646`.

D. B. Kilgour, G. A. Novak, J. S. Sauer, A. N. Moore, J. Dinasquet, S. Amiri, E. B. Franklin, K. Mayer, M. Winter, C. K. Morris, T. Price, F. Malfatti, D. R. Crocker, C. Lee, C. D. Cappa, A. H. Goldstein, K. A. Prather, and T. H. Bertram. Marine gas-phase sulfur emissions during an induced phytoplankton bloom. *Atmos Chem Phys*, 22:1601–1613, 2022. doi: https://doi.org/10.5194/acp-22-1601-2022.

J. Krechmer, F. Lopez-Hilfiker, A. Koss, M. Hutterli, C. Stoermer, B. Deming, J. Kimmel, C. Warneke, R. Holzinger, J. Jayne, D. Worsnop, K. Fuhrer, M. Gonin, and J. de Gouw. Evaluation of a new reagent-ion source and focusing ion–molecule reactor for use in proton-transfer-reaction mass spectrometry. *Analytical Chemistry*, 90(20):12011–12018, 2018. ISSN 0003-2700. doi: 10.1021/acs.analchem.8b02641. URL `https://doi.org/10.1021/acs.analchem.8b02641`.

F. Li, D. D. Huang, L. Tian, B. Yuan, W. Tan, L. Zhu, P. Ye, D. Worsnop, K. I. Hoi, K. M. Mok, and Y. J. Li. Response of protonated, adduct, and fragmented ions in vocus proton-transfer-reaction time-of-flight mass spectrometer (ptr-tof-ms). *Atmospheric Measurement Techniques*, 17(8):2415–2427, 2024. doi: 10.5194/amt-17-2415-2024. URL `https://amt.copernicus.org/articles/17/2415/2024/`.

M. P. Vermeuel, D. B. Millet, D. K. Farmer, M. A. Pothier, M. F. Link, M. Riches, S. Williams, and L. A. Garofalo. Closing the Reactive Carbon Flux Budget: Observations From Dual Mass Spectrometers Over a Coniferous Forest. *Journal of Geophysical Research: Atmospheres*, 128(14): e2023JD038753, July 2023. ISSN 2169-897X, 2169-8996. doi: 10.1029/2023JD038753. URL `https://agupubs.onlinelibrary.wiley.com/doi/10.1029/2023JD038753`.

L. Xu, M. M. Coggon, C. E. Stockwell, J. B. Gilman, M. A. Robinson, M. Breitenlechner, A. Lamplugh, J. D. Crounse, P. O. Wennberg, J. A. Neuman, G. A. Novak, P. R. Veres, S. S. Brown, and C. Warneke. Chemical ionization mass spectrometry utilizing ammonium ions (nh4+ cims) for measurements of organic compounds in the atmosphere. *Atmospheric Measurement Techniques*, 15(24):7353–7373, 2022. ISSN 1867-8548. doi: 10.5194/amt-15-7353-2022.